① −31

- Since none of the particle-type bulk bands are mixed with hole-type bulk bands during the interpolation between $\lambda = 0$ and $\lambda = 1$, the sum of the Chern integer over particle-type bands does not change during $\lambda = 1$ to $\lambda = 0$:

$$\sum_{n=1}^{N} ch_n(\lambda = 1) = \sum_{n=1}^{N} ch_n(\lambda = 0). \quad \text{(A-22)}$$

- At $\lambda = 0$, $H(\mathbb{k}, \lambda)$ is trivially diagonalized by a unit matrix, so that the r.h.s. is zero for every n.

- Thus the l.h.s. is also zero, due to this invariance.

- This sum rule suggests that, unlike fermion ~~c~~ cases (TR-breaking topological superconductor), usual quasi-particle topological boson systems do not have any those topological edge (boundary) modes, which connect the particle-type bulk bands and the hole type-bulk bands.

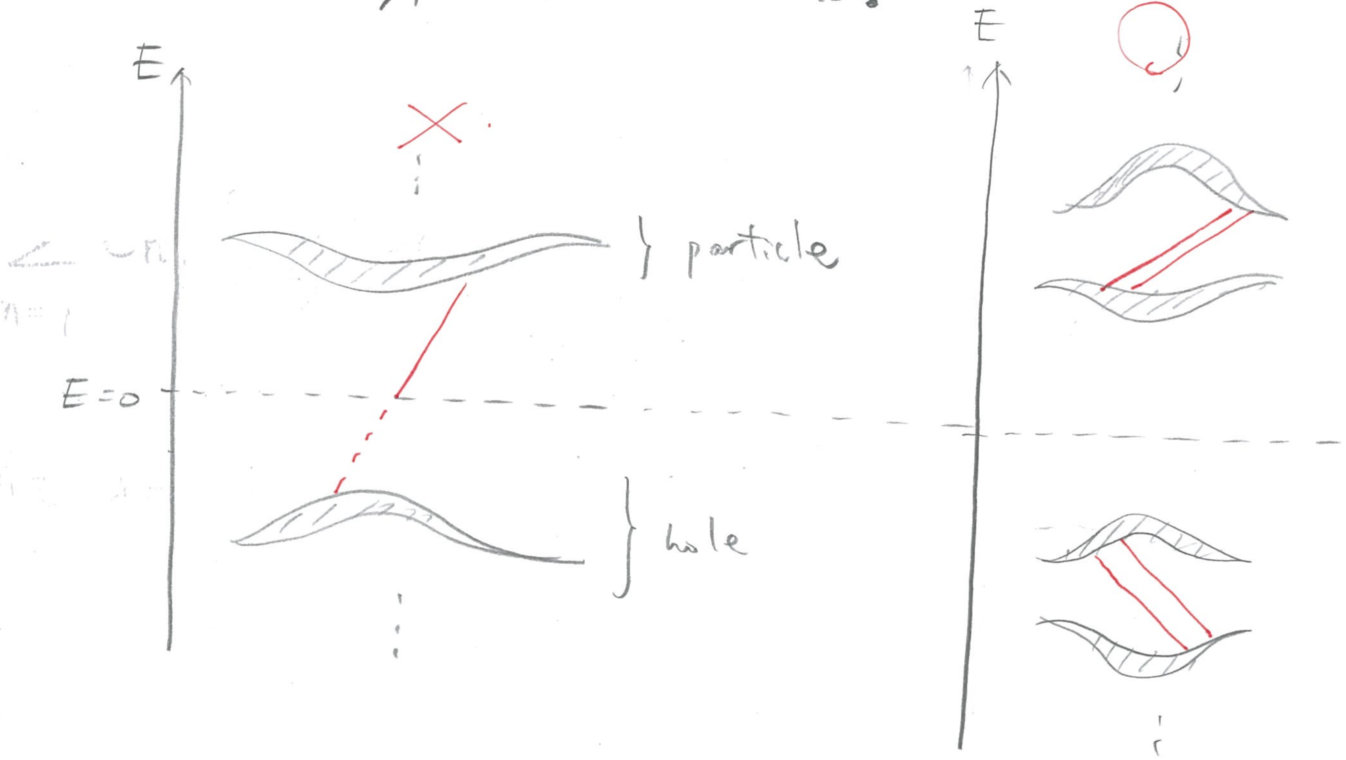

Instead, topological edge modes appear only in a finite frequency regime.

- To relate these topological modes with the topological integer defined by the paraunitary transformation, let us again use the previous interpolation. (1)-33

- Let us begin with $\lambda = 0$, where all the Chern integers are zero.

When finite λ is gradually introduced, N-fold degenerate particle-type bands will be split into N non-degenerate dispersive bands.

- Thereby, we can define chern integers for each bands.

- When λ is small enough, $H_{2N \times 2N}(k, \lambda)$ has a little k-dependence and so does $T_k(\lambda)$. As such, the quantized quantity like the Chern integer remains still zero for every band.

- When λ further grows up, there appears a band crossing between neighboring particle-type bands.

- Suppose that the crossing appears at $\lambda = \lambda_c$ and it is between n-th particle-type band and $(n+1)$-th band.

- For $\lambda < \lambda_c$ and for $\lambda > \lambda_c$, the n-th band has no degeneracy with the others, so that the Chern integer for the band are quantized to be integers.

$$\begin{cases} Ch_n(\lambda > \lambda_c) = n \\ ch_n(\lambda < \lambda_c) = 0 \end{cases} \quad \text{— (A-23)}$$

- The difference between these two can be given by a surface integral of a dual magnetic field over a closed surface in the k_x-k_y-λ space, which encloses the band crossing point at $(\mathbb{k}, \lambda) = (\mathbb{k}_c, \lambda_c)$:

$$\mathrm{ch}_n(\lambda > \lambda_c) - \mathrm{ch}_n(\lambda < \lambda_c) = \frac{1}{2\pi} \int_S d\vec{S} \cdot \vec{B}_n \quad \text{(A-24)}$$

where

$$\begin{cases} \vec{B}_n(\mathbb{k}, \lambda) \stackrel{d}{\equiv} (\partial_{k_x}, \partial_{k_y}, \partial_\lambda) \times \vec{A}_n(\mathbb{k}, \lambda) \\ \vec{A}_n(\mathbb{k}, \lambda) \stackrel{d}{\equiv} i\,\mathrm{Tr}\left[\Gamma_n \hat{\sigma}_3 T^\dagger_{\mathbb{k}} \hat{\sigma}_3 (\vec{\nabla} T_{\mathbb{k}})\right] \\ \vec{\nabla} \stackrel{d}{\equiv} (\partial_{k_x}, \partial_{k_y}, \partial_\lambda). \end{cases} \quad \text{(A-25)}$$

and S is a closed surface, inside which the band crossing at $(\mathbb{k}, \lambda) = (\mathbb{k}_c, \lambda_c)$ is included.

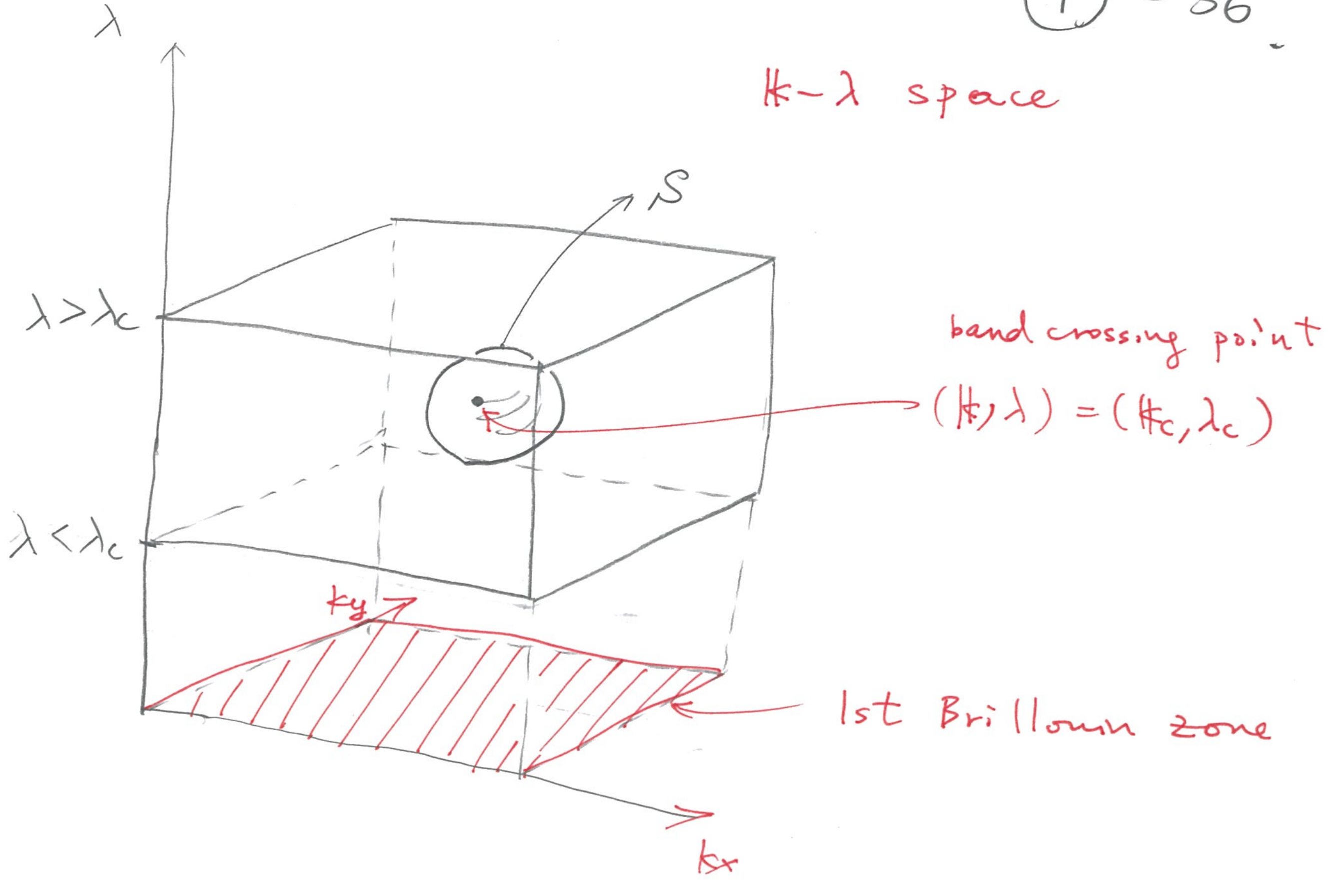

(r.h.s.) of eq. (A-24)

$$= \frac{1}{2\pi}\int_{\text{B.Z. at } \lambda>\lambda_c} dk_x dk_y \cdot B_{n,\lambda} - \frac{1}{2\pi}\int_{\text{B.Z. at } \lambda<\lambda_c} dk_x dk_y\, B_{n,\lambda}$$

$$= \frac{1}{2\pi}\int_{\square} d\vec{S}\cdot\vec{B} = \frac{1}{2\pi}\int_{S} d\vec{S}\cdot\vec{B}$$ for $\forall S$ which includes $(\mathbb{k}_c,\lambda_c)$.

($\because$ $\vec{B}(\mathbb{k},\lambda)$ is a periodic function of $\mathbb{k}$ with the B.Z.)

- Eq. (A-24) holds true for an <u>arbitrary</u> S which includes the band touching point at $(\mathbb{k},\lambda)=(\mathbb{k}_c,\lambda_c)$

- Thus, we can make it sufficiently small, so that $(\mathbb{k},\lambda)$ on S is sufficiently proximate to $(\mathbb{k}_c,\lambda_c)$.

- For such $(\mathbb{k},\lambda)$, $\vec{B}_n(\mathbb{k},\lambda)$ can be determined <u>only</u> by an effective 2×2 Hamiltonian for the n-th band and $(n+1)$-th band.

- To see this, suppose that $H(\mathbb{k}_c,\lambda_c)$ is diagonalized by an paraunitary matrix Π_0

$$\Pi_0^{\dagger}\cdot \overbrace{H(\mathbb{k}_c,\lambda_c)}^{H_0}\cdot \Pi_0$$

$$= \begin{array}{c} \begin{array}{cc} \quad\quad\quad\; n & n+1 \\ \quad\quad\quad\;\downarrow & \downarrow \end{array} \\ \left(\begin{array}{cccc|c} \ddots & & & & \\ & E_0 & & & \\ & & E_0 & & \\ & & & \ddots & \\ \hline & & & & \ddots \end{array}\right) \end{array} \begin{array}{l} \left.\vphantom{\begin{array}{c}1\\1\\1\\1\end{array}}\right\} p \\ \left.\vphantom{1}\right\} h \end{array} \quad \text{(A-27)}$$

- where we assume that $-\mathbb{k}_c \neq \mathbb{k}_c$ under modulo Brillouin zone, so that the degeneracy appears only in the n-th particle-type band and (n+1)-th particle band.

- For the case with $-\mathbb{k}_c = \mathbb{k}_c$, one can easily generalize the following argument, so that I will omit this.

- For $(\mathbb{k}, \lambda)$ proximate to $(\mathbb{k}_c, \lambda_c)$, we could expand $H(\mathbb{k}, \lambda)$ around H_0

$$\hat{H}(\mathbb{k}, \lambda) \equiv \hat{H}_0 + \hat{V}_{\mathbb{p}} \qquad \text{—— (A-28)}$$

where $\mathbb{p} \overset{\mathrm{def}}{\equiv} (\mathbb{k}, \lambda) - (\mathbb{k}_c, \lambda_c)$ and $\hat{V}_{\mathbb{p}}$ is at most the first order in small $\mathbb{p}$.

- Then, at the leading order in small $\mathbb{p}$, $H(\mathbb{k}, \lambda)$ can be diagonalized by a product between $\hat{\mathbb{T}}_0$ and a unitary transformation $\hat{U}_{\mathbb{P}}$;

$$\mathbb{T}_p = \hat{\mathbb{T}}_0 \hat{U}_{\mathbb{P}} + O(\mathbb{P}) \qquad \text{—(A-29)}$$

- where $\hat{U}_{\mathbb{P}}$ diagonalizes the effective 2×2 Hamiltonian given by n-th and (n+1)-th column vectors of $\hat{\mathbb{T}}_0$;

$$\hat{\mathbb{T}}_0 \overset{\text{def}}{\equiv} \Big(\underbrace{\cdots \; \vec{t}_n \; \vec{t}_{n+1} \; \cdots}_{P} \;\Big|\; \underbrace{\qquad\qquad}_{h} \Big) \qquad \text{—(A-30)}$$

$$H^{\text{eff}}_{2\times 2} \equiv \begin{pmatrix} \vec{t}_n^{\,\dagger} \cdot \hat{V}_{\mathbb{P}} \cdot \vec{t}_n & \vec{t}_n^{\,\dagger} \cdot \hat{V}_{\mathbb{P}} \cdot t_{n+1} \\ \vec{t}_{n+1}^{\,\dagger} \cdot \hat{V}_{\mathbb{P}} \cdot \vec{t}_n & \vec{t}_{n+1}^{\,\dagger} \cdot \hat{V}_{\mathbb{P}} \cdot t_{n+1} \end{pmatrix} \qquad \text{—(A-31)}$$

- Note that $H^{\text{eff}}_{2\times 2}$ is on the 1st order in small $\mathbb{P}$, while $\hat{U}_{\mathbb{P}}$ which diagonales this is on the zero-th order in small $\mathbb{p}$.

- Since $\hat{U}_{\mathbb{p}}$ commutes with σ_3, we can rewrite eq. (A-25) only in terms of $\hat{U}_{\mathbb{p}}$ at the leading order in small $\mathbb{p}$:

$$\begin{cases} \vec{B}_n(\mathbb{p}) = \vec{\nabla} \times \vec{A}_n(\mathbb{p}) + o\left(\frac{1}{|\mathbb{p}|}\right). \quad (A-32) \\ \vec{A}_n(\mathbb{p}) = i\,Tr\left[P_n \hat{\sigma}_3 U_{\mathbb{p}}^{\dagger} \cancel{T_0^{\dagger} \sigma_3 T_0} (\vec{\nabla} U_p) \right] \\ \qquad = i\,tr\left[U_{\mathbb{p}}^{\dagger} \vec{\nabla} \vec{U}_p \right] \quad (1 \leq n \leq N) \end{cases}$$

- Note that the leading order is on the order of $\left(\frac{1}{|\mathbb{p}|^2}\right)$ in small $|\mathbb{p}|$, while the sub-leading order in (A-32) comes from the $O(|\mathbb{p}|)$ contribution in the r.h.s. of eq. (A-29).

- When S (the sphere which encloses the band touching point) is chosen to be sufficiently small, we see that the r.h.s. (of eq. (A-24)) is determined only by the unitary transformation which diagonalize the 2 × 2 effective Hamiltonian $H^{eff}_{2\times 2}$:

- Following the same argument as in the fermion case; Oshikawa PRB 50 17357 (1994), the r.h.s. of eq. (A-24) is shown to be given as,

$$ch_n(\lambda > \lambda_c) - ch_n(\lambda < \lambda_c) = \underbrace{\mathrm{sgn}(\det \hat{V})}_{\text{magnetic charge.}}$$

with a real valued 3 × 3 matrix $\hat{V}$;

$$\hat{H}^{eff}_{2\times 2}(p) = \sum_{\mu,\nu=1}^{3} p_\mu V_{\mu\nu} \hat{\sigma}_\nu \quad \text{— (A-33)}$$

2 × 2 Pauli matrix

(e.g. Oshikawa. PRB 50 17357 (1994).)

Likewise, following the Fermion's case,

- Su, Schrieffer, Heeger PRL 42 1698 (1979)
- Niemi and Semenoff Phys. Rep. 135 99 (1986)

We can show that the band gap between these two bulk bands acquire one chiral edge modes after $\lambda > \lambda_c$, and that the group velocity of the chiral mode is determined by the sign of this magnetic charge:

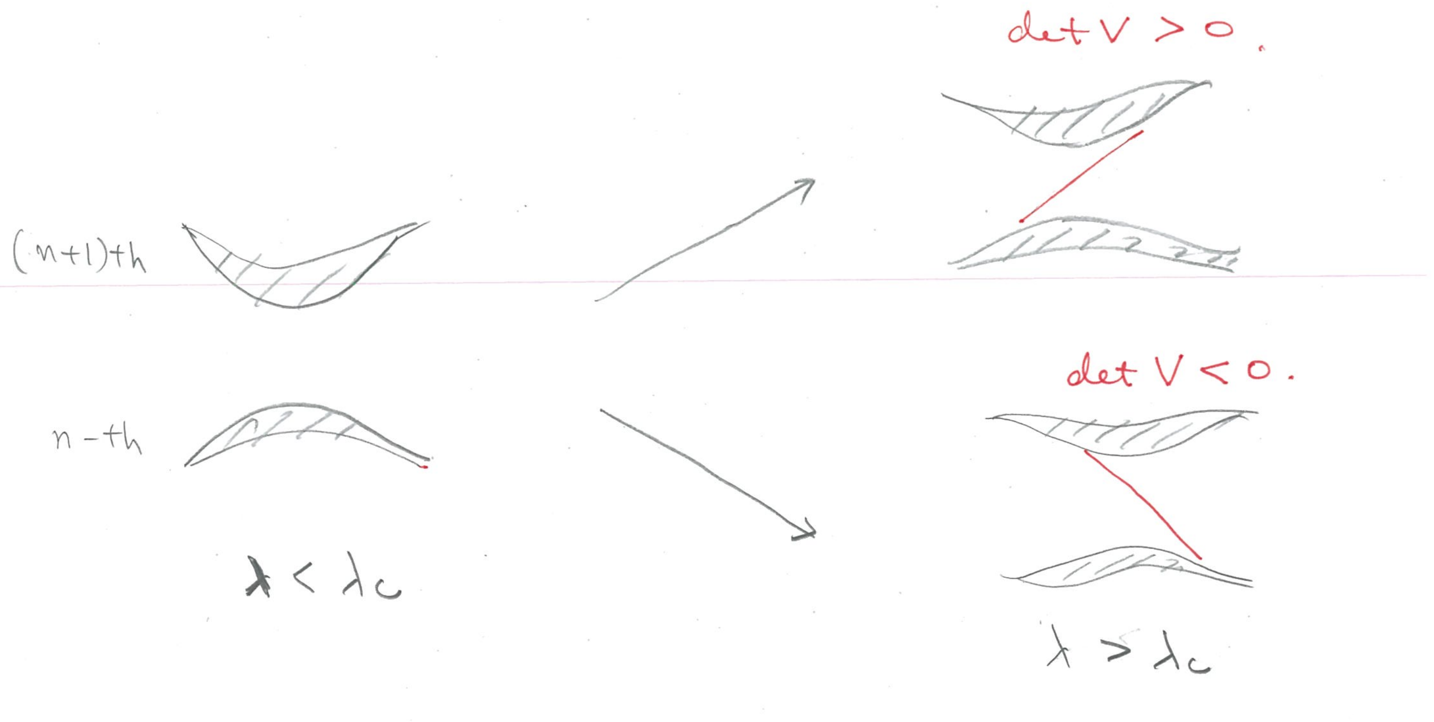

Therefore, integrating these observations from $\lambda = 0$ to $\lambda = 1$, we can argue that the number of chiral edge modes (with sign) which go across an energy E is equal to a sum of the Chern integer over those particle-type bulk bands whose energy is smaller than E.

$$\#\left(\text{chiral edge modes at } E\right) = \sum_{n}^{0 < E_n < E} ch_n$$

3 Physical systems (mainly about magnons).

- What kind of physical systems can realize topological quasi-particle boson excitations?

- From symmetry point of view, the BdG Hamiltonian needs to break both time-reversal symmetry,

$$H(\mathbb{k}) \neq H^*(-\mathbb{k}).$$

$$\left(\Omega^{xy}_{n,\mathbb{k}} \neq -\Omega^{xy}_{n,-\mathbb{k}} \right)$$

and mirror symmetries. (σ_x or σ_y)

$$H(k_x, k_y) \neq H(-k_x, k_y)$$

$$\neq H(k_x, -k_y)$$

$$\left(\begin{aligned} \Omega^{xy}_{n,(k_x,k_y)} &\neq -\Omega^{xy}_{n,(-k_x,k_y)} \\ &\neq -\Omega^{xy}_{n,(k_x,-k_y)} \end{aligned} \right)$$

- In a system with quasi-particle boson excitations such as (photon, phonon, magnon, ..)

these broken symmetries can be most easily realized by a ferromagnetic or ferrimagnetic moment M_z along the out-of-plane direction, (along the z-direction)

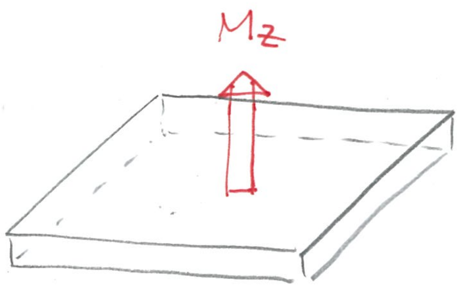

$$\hat{M}_z \rightarrow -\hat{M}_z$$

(· time-reversal.
· mirror symmetries
($x \to -x$ or $y \to -y$).)

$$\hat{M}_z \sim x \cdot \hat{p}_y - \hat{y} \hat{p}_x$$

$$(\ \sigma_x \equiv I \cdot R_x^{\pi}, \quad \sigma_y \equiv I \cdot R_y^{\pi}\ )$$

- Meanwhile, some of these symmetries are still preserved by an in-plane ferromagnetic moment

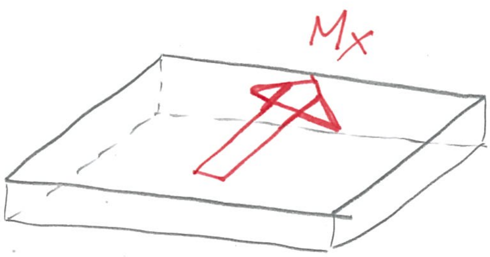

$$M_x \rightarrow M_x$$

$$\sigma_x \equiv I \cdot R_x^{\pi}$$

$$\hat{M}_x \sim y \hat{p}_z - z \hat{p}_y \ .$$

- From the microscopic point of view, a system needs to have <u>coupling</u> between the magnetic moment and spatial coordinate.

- Otherwise, the ferromagnetic moment flipped by these symmetries can be further flipped back to its original direction by a rotation in spin.

e.g.)

- Without any coupling between moment and spatial coordinate

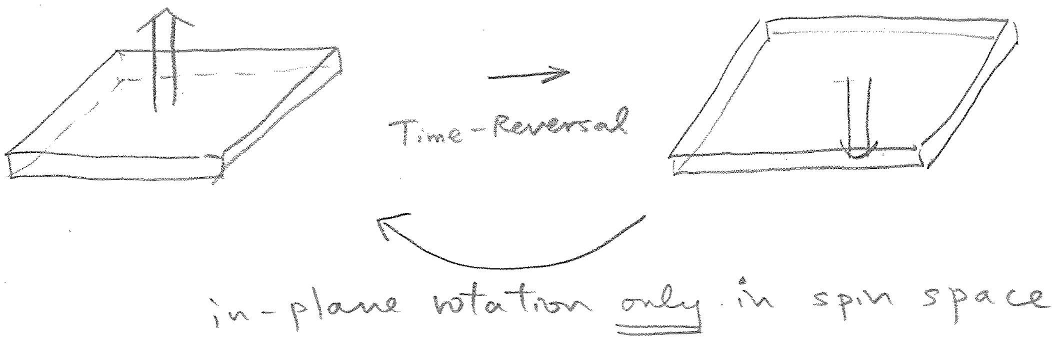

$$\Rightarrow \quad H^*(\mathbb{k}) = H(-\mathbb{k})$$

$$\Rightarrow \quad \Omega^{xy}_{n,\mathbb{k}} = -\Omega^{xy}_{n,-\mathbb{k}}$$

$\Rightarrow$ Chern integer becomes zero even in the presence of M_z.

• With the coupling between $\begin{pmatrix} \text{magnetic moment} \\ \text{spatial coordinate} \end{pmatrix}$

① -47

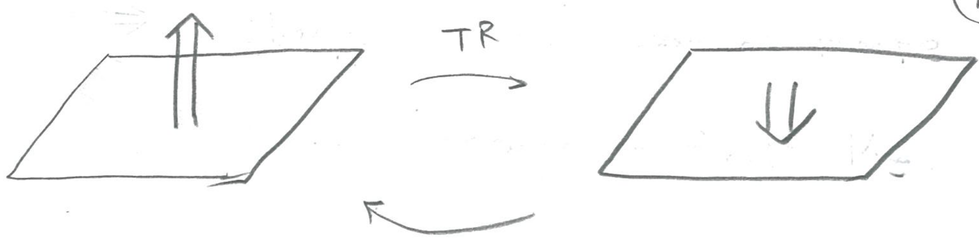

in-plane rotation both in $\begin{pmatrix} \text{spin space} \\ \text{spatial coordinate space} \end{pmatrix}$

$$\Rightarrow \quad H^*(k_x, k_y) = H(-k_x, k_y) = H(k_x, -k_y)$$

$$\Rightarrow \quad \Omega^{xy}_{n,}(k_x, k_y) = \Omega^{xy}_{n,}(-k_x, k_y) = \Omega^{xy}_{n,}(k_x, -k_y)$$

$\Rightarrow$ Chern integer can be finite in the presence of finite M_z

• Spin-orbital locking interaction in nature.

⊙ Maxwell equation in continuous media

$$\begin{cases} \underline{\nabla \cdot \mathbb{B}}(\mathbf{x}, t) = 0, & \nabla \times \mathbb{E}(\mathbf{x}, t) + \frac{1}{c}\frac{\partial \mathbb{B}(\mathbf{x}, t)}{\partial t} = 0 \\ \nabla \cdot \mathbb{D}(\mathbf{x}, t) = \rho, & \underline{\nabla \times \mathbb{H}}(\mathbf{x}, t) - \frac{1}{c}\frac{\partial \mathbb{D}(\mathbf{x}, t)}{\partial t} = \frac{1}{c}\overset{\circ}{\mathbb{J}} \end{cases}$$

where $\mathbb{B} = \mathbb{H} + 4\pi \underbrace{\mathbb{M}}_{\text{magnetic moment}}$

inner product between $\mathbb{M}$ and spatial coordinate.

⊙ effective boson-boson interactions induced by relativistic spin-orbit interaction ①-48

Dzyloshinskii-Moriya (DM) interaction.

or anisotropic spin exchange interactions in Mott insulators with larger relativistic effect (iridate, ruthenate, ...)

$$\begin{cases} \cdot\ \vec{D}_\mu \cdot (\vec{M} \times \nabla_\mu \vec{M}) & \text{DM interaction.} \\ \cdot\ \sum^{\text{space}}_{\mu,\nu} \sum^{\text{spin}}_{\alpha,\beta} (\nabla_\mu M_\alpha) \cdot T^{\mu}_{\alpha\beta} (\nabla_\mu M_\beta) & \end{cases}$$

(symmetric part of) anisotropic spin exchange interaction.

· Topological Magnons ?

· Magnon (spin wave) is a collective propagation of magnetic moment.

$$\begin{cases} \dfrac{\partial \mathbf{M}}{\partial t} = -\gamma \mathbf{M} \times \mathbf{H}_{\mathrm{eff}} \qquad \vec{D}_\mu \\ \mathbf{H}_{\mathrm{eff}} = \underbrace{\vec{H}_d}_{\text{dipolar field}} + \underbrace{\lambda_{ex}^{-2} \nabla^2 \vec{M} + \lambda_{DM}^{-1} (\vec{n}_\mu \times \nabla_\mu \vec{M})}_{\text{exchange fields}} + \cdots \end{cases}$$

$$\begin{cases} \nabla \cdot (\mathbb{H}_d + 4\pi \mathbb{M}) = 0 \\ \nabla \times \mathbb{H}_d = 0 \end{cases}$$

magnetostatic approximation

(speed of light >> spin wave velocity)

$\Rightarrow$ dipolar field $\mathbb{H}_d(\mathbf{r})$ in terms of $\mathbb{M}(\mathbf{r})$

$$\mathbb{H}_d(\mathbf{r}) = \frac{1}{4\pi} \int d\mathbf{r}' \left\{ \frac{\mathbb{M}(\mathbf{r}')}{|\mathbf{r}-\mathbf{r}'|^3} - 3 \frac{(\mathbf{r}-\mathbf{r}')(\mathbf{r}-\mathbf{r}')\cdot\mathbb{M}(\mathbf{r}')}{|\mathbf{r}-\mathbf{r}'|^5} \right\}$$

- Due to the spin-orbital locking in the Maxwell equation, the dipolar field contains the inner product between $\mathbb{M}(\mathbf{r}')$ and spatial coordinate $(\mathbf{r}-\mathbf{r}')$

- λ_{ex}, λ_{DM} and ... have a length scale, over which these interactions range spatially.

- Such length is usually on the order of the atomic scale.

• when the wavelength of spin wave in much longer than these atomic scale length, the (1)-50 dipolar field $H_d(\mathbf{r})$ become a dominant driving force of spin wave.

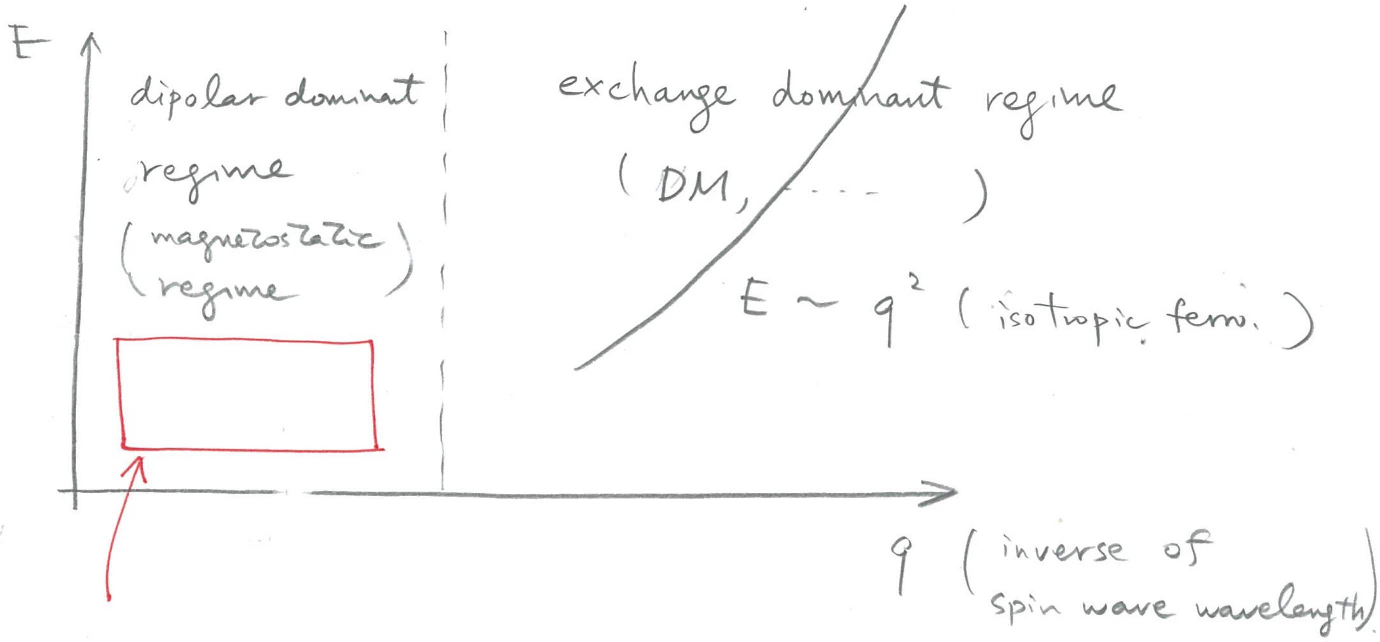

• dispersion depends on shape of sample, direction of ferromagnetic moment

(Walker, Kittel, Damon, Eshbach, ..)

⇒ topological magnons in dipolar regimes

RS, Matsumoto, Ohe, Murakami, Saitoh

PRB <u>87</u> 174427 (2013)

PRB <u>87</u> 174402 (2013)

PRB <u>89</u> 054412 (2014)

- topological magnons in exchange regime

①-51

Lifa Zhang, Ren, Wang, Li

PRB 87 144101 (2013)

- Resonance frequency regime

$$\begin{cases} \text{dipolar spin wave} & (\text{GHz / Microwave}) \\ \text{exchange spin wave} & (\text{THz}) \end{cases}$$

- Standard experimental method for studying dipolar spin waves is microwave experiment with coplanar waveguides.

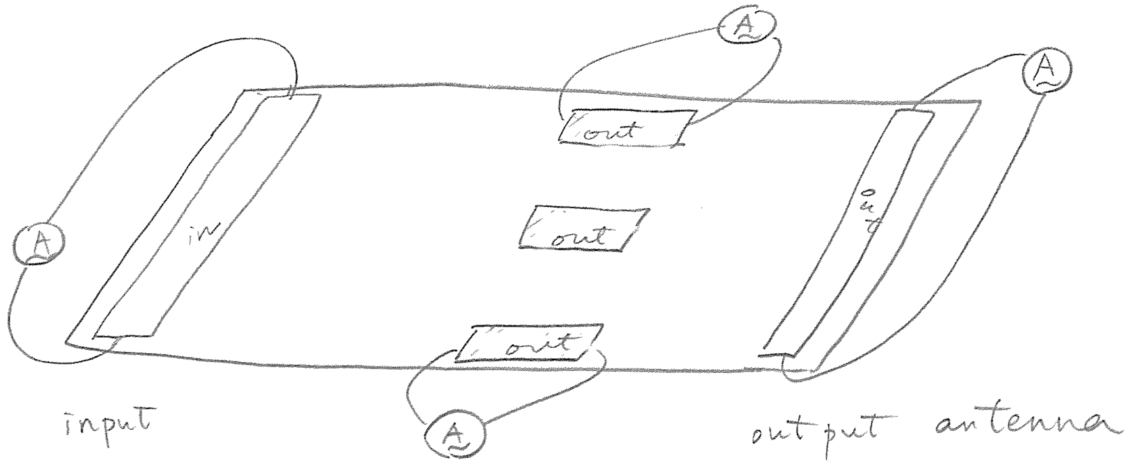

- AC electric current in input antenna excites spin waves. Spin waves propagate spatially, to reach around output antenna, inducing ac current in the output antenna.

⇛ Useful to detect topological magnons directly.

• Another experiment which can indirectly detect topological magnons is thermal Hall conductivity

$$K_{xy} \equiv -\frac{k_B^2 T}{hV} \sum_{\mathbb{k}} \left(c_2[g(\epsilon_{n,\mathbb{k}})] - \frac{\pi^2}{3} \right) \Omega^{xy}_{n,\mathbb{k}}$$

$$\left(\text{where} \quad g(x) = \frac{1}{e^{\beta x}-1}, \; c_2[x] \equiv \int_0^x dt \left[\ln\left(\frac{1+t}{t}\right) \right]^2 \right)$$

• Matsumoto, Murakami PRL $\underline{106}$ 197202 (2011)

PRB $\underline{84}$ 184406 (2011)

⇒ Matsumoto, RS, Murakami PRB $\underline{89}$ 054420 (2014)

Qin, Niu, Shi PRL $\underline{107}$ 236601 (2011)

Qin, Zhou, Shi PRB $\underline{86}$ 104305 (2012)